

# Assessing the Interplay between Localization Accuracy and Interference in IRS-assisted Links

Jorge Torres Gómez, and Falko Dressler

School for Electrical Engineering and Computer Science, TU Berlin, Berlin, Germany

Email: {torres-gomez, dressler}@ccs-labs.org

**Abstract**—This paper assesses the localization capabilities in intelligent reflective surface (IRS)-assisted links within a multiple mobile user (MU) scenario. The localization is performed by scanning a given area where the MU is located and measuring the receiver power from transmissions. The scanning is performed by configuring the IRS beam to target a given location in the ground plane. The base station (BS) will render the received power with the coordinates of the IRS beam and estimate the MU location with the peak in the power surface. We also include a factor of hardware impairment in calculating the power at the BS. This factor accounts for a realistic implementation of the communication scheme and the non-linearities in the radio frequency (RF) front end. Our simulation results demonstrate the achievable localization error in the centimeter scale with the amount of interfering mobile users.

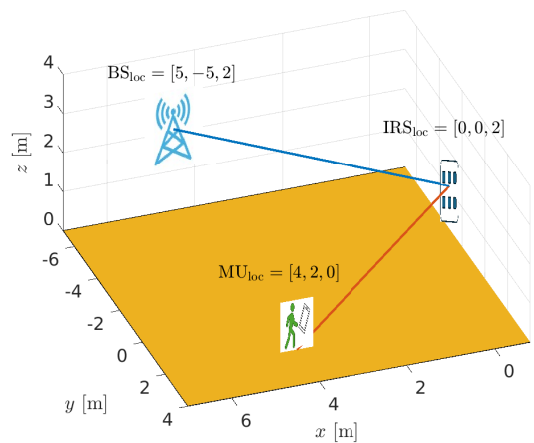
**Index Terms**—Intelligent reflective surfaces, IRS, localization, mobile users

## I. INTRODUCTION

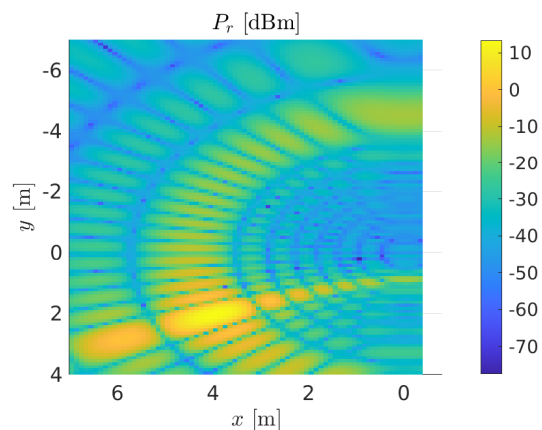
Intelligent reflective surface (IRS)-assisted links are a promising means to realize enhanced communication links avoiding obstacles at a low cost of deployment. Especially in the mmWave and sub-THz bands, IRSs are particularly functional as these links are more vulnerable to obstacles like walls or furniture [1]. In this way, applications like wireless localization further extend their reachability into areas with limited connectivity. Applications stem toward the ubiquitous support for indoor navigation, intelligent transportation systems, or healthcare as an ongoing trend in fifth generation (5G) and sixth generation (6G) communication systems [2]. IRS in general, but particularly coordination in 6G multi-operator IRS-assisted networks [3] requires accurate user localization.

Leveraging on IRS-assisted links, localization schemes identify targets by detecting their radio pattern with respect to the coordinates. Algorithms estimate the distance from targets by through signal parameters like the received signal strength (RSS), the time of flight (ToF), or the angle of arrival (AoA) [4]. Most of the reported solutions implement the maximum likelihood estimator (MLE) [5]–[7] and also derive theoretical bounds on the localization error performance with the Cramer-Rao lower bound (CRLB) [5], [6], [8]. Furthermore, the location estimation is also reported through a data-driven approach with supervised learning [2].

In this paper, we consider the use case depicted in Fig. 1a, where a BS attempts to localize a MU in the  $x$ - $y$ -plane. We assume the MU has non-line of sight (NLoS) connection with



(a) Schematic representation of deployed base station (BS), IRS, and mobile user (MU).



(b) Received power level at the BS when the MU is located at coordinates (4, 2, 0).

Fig. 1. Schematic representation of the communication scheme and received power at the BS.

the BS and a communication link is only conceived via the IRS. The BS will reconfigure the IRS to scan in the  $x$ - $y$ -plane along smaller blocks, rendering the receiver power with the block location. For instance, when the MU is located with the coordinates [4, 2] in the  $x$ - $y$ -plane, the BS will profile a power distribution as illustrated in Fig. 1b. As we observe from this figure, there is a direct correspondence between the MU location and the power level, which is used to estimate the MU position.

At the BS, we estimate the MU position, looking for the maximum of the received power. This RSS-based solution strives for a low complex method that we illustrate performs with localization errors in the centimeter (cm) scale. Besides, we also consider the case of multiple MUs randomly located in the  $xy$ -plane to evaluate the localization performance.

We also evaluate a multiple MUs scenario, where we assume the target MU sends a unique code in the form of a preamble that can be later identified at the BS. This way, we distinguish the signal from the target MU through a cross-correlation procedure. To be more realistic, we also assume some leakage power from neighbors MU in detecting the target one. This power leakage can be related to hardware impairments such as non-linearities of the amplifiers and converters in the radio frequency (RF) front end, which allows for evaluation aside from ideal assumptions [9].

Our key contributions can be summarized as follows:

- We provide a methodology to localize the received power at a BS with the RSS of the MUs emissions, and
- We illustrate performance with the localization errors of the target MU.

## II. RELATED WORK

IRS-assisted links extend the reachability to localize targets while circumventing obstacles. With the inclusion of IRSs elements, the MUs can be localized better by the BSs, as a direct line of sight (LoS) link is established with the MUs. Solutions implement localization detecting parameters in the transmission of Orthogonal Frequency Division Multiplexing (OFDM) signals [5], [7], [10], [11] or single pilot tones as in [1], [12]. Transmissions are performed in the GHz band as the case in [12], and in the sub-mmWave band at 28 GHz as in [5], [10].

Most reported localization algorithms are based on the MLE method [5]–[7]. Based on this formulation, distance-dependent parameters are estimated from the received signal, which localizes the source of emissions. Besides, not only the localization of targets is performed, but also the orientation of the target’s antenna as addressed in [5].

Performance is evaluated through simulations accounting for the root mean squared error (RMSE) of the localization errors. The RMSE is derived with various parameters such as the distance of the target MU from the IRS [6], the number of pilot tones [10], the signal to noise ratio (SNR) of the received signal [7], and also accounting for the number of IRS’s elements and MU in the grid [12]. Theoretical expressions also evaluate the CRLB accounting for the minimum localization errors, as described in [5], [6], [8].

Realistic assumptions are also included to evaluate the localization errors. The impact of quantization on the localization performance is evaluated in [8]. The amplitude and the phase of the IRS are defined in a finite set, in this way restricting the IRS beam to a finite amount of configurations. Hardware impairments can also be considered in modeling the recovered signal [9]. Hardware impairments include non-linearities in the amplification chain, phase imbalance in the

mixers, and the finite resolution of analog-to-digital converters. This unavoidable effect on the RF front end degrades the estimation of signal parameters due to the introduced distortion.

In this paper, we visualize the localization performance and consider hardware impairments. When localizing the target one, we introduce this impairment to model the leakage power from neighbors MU emissions. This impairment is interpreted as a leakage power interfering with detecting the target MU.

## III. SYSTEM MODEL

We consider a communication system comprised of a BS, an IRS, and multiple MUs. We evaluate the most challenging scenario when there are NLoS conditions between the MUs and the BS. We assume fixed locations for the IRS and the BS, as illustrated in Fig. 1a. The MUs will be located in the  $xy$ -plane with arbitrary coordinates and total numbers.

Each MU will emit a signal  $s_i(t)$  of the same power 30 dBm and at frequency of 28 GHz. The BS will receive the transmitted signal by the MUs via the IRS, as we assume NLoS conditions between the MUs and the IRS. We assume free-space conditions for the channel, where the received signal is given by [13, Eq. (7)]

$$r(t) = w \times \sum_{i=1}^{N_u} s_i(t) + n(t) \quad (1)$$

where  $n(t)$  is the additive white gaussian noise (AWGN) at the BS and  $w$  is the channel gain in the link IRS assisted link between the MU and the BS as

$$w = \frac{G_{\text{MU}} G_{\text{IRS}} G_{\text{BS}} A_{\text{BS}} A_{\text{IRS}}}{4\pi} \times \sum_{n=1}^N \frac{\sqrt{F_n} \hat{\theta}_n}{d_{\text{MU},n} d_{\text{BS},n}} e^{-\frac{j2\pi(d_{\text{MU},n} + d_{\text{BS},n})}{\lambda}}, \quad (2)$$

comprising the antenna’s radiation properties of the MU, IRS, and MU, as well as the corresponding distances. The system parameters are described in Table I (we follow the concepts in [13]), while the distances are given between each  $n$ -th element of the IRS with the BS, as given by  $d_{\text{MU},n}$ , and with the MU, as given by  $d_{\text{BS},n}$ .

In particular, the coefficient  $\hat{\theta}_n$  stands for reflection coefficients of the IRS. This coefficient links an arbitrary location in the  $x$ - $y$ -plane with the BS. The next section elaborates further on its calculation.

We assume each MU implements a preamble with their transmission as an identifier known at the BS. The BS will receive the superposition of all transmissions but will identify the intended MU when cross-correlating the transmissions with the stored preamble at the BS. The highest cross-correlation will identify the intended MU.

Aiming to conceive a realistic implementation, we assume some power leakage in the cross-correlation operation with the others MUs. In this respect, we will assume an  $\alpha$  coefficient in the range  $[0, 1]$ , where  $\alpha = 1$  denotes the worst case, indicating that all the power from other MUs leaks into the detection of the actual one.

TABLE I  
SYSTEM PARAMETERS.

Parameter	Description	Value
$L \times W$	Area size in the $x$ - $y$ -plane	$4 \times 4$ m
$\text{IRS}_{\text{loc}}$	IRS coordinates	$[0, 2, 0]$ m
$N_h \times N_v$	IRS total elements	$25 \times 25$
$P_{\text{BS}}$	Power at the BS	30 dBm
$G_{\text{BS}}$	Antenna gain at the BS	21 dBm
$F_{\text{BS}}$	Radiation pattern of the transmit antenna	1
$A_{\text{BS}}$	Aperture of the BS antenna	$\frac{\lambda^2}{4\pi}$
$\text{BS}_{\text{loc}}$	BS coordinates	$[5, 2, 0]$ m
$P_{\text{MU}}$	Power at the MU	30 dBm
$G_{\text{MU}}$	Antenna gain at the MU	21 dBm
$F_{\text{MU}}$	Radiation pattern of the transmit antenna	1
$A_u$	Aperture of the transmit antenna	$\frac{\lambda^2}{4\pi}$
$\text{MU}_{\text{loc}}$	BS coordinates	$[5, -5, 2]$ m

#### IV. TARGET LOCALIZATION

We localize the MU by looking at the power level of the received signal at the BS. The received power at the BS will be the one in the LoS link with the IRS, configured to point to a given location in the  $xy$ -plane. Whenever this location matches the MU position, we will observe a peak amplitude, as depicted in Fig. 1b.

The localization algorithm is quite straightforward to implement. Given an area of size  $L_x \times L_y$ , we divide the area into a grid of size  $\delta$ , giving a total of  $N_b = \frac{L_x}{\delta} \times \frac{L_y}{\delta}$  blocks. Then, given this block, we implement the following algorithm:

---

**Algorithm 1** Algorithm to localize the MU

---

**Ensure:**  $x_{\text{peak}} = 0, y_{\text{peak}} = 0, P_{\text{peak}} = 0$

- 1: **while**  $n \leq N_b$  **do**
  - 2:     Configure the IRS to point to the location  $(x_n, y_n)$
  - 3:     Compute the received power at the BS and saved it in  $P_r$
  - 4:     **if**  $P_r > P_{\text{peak}}$  **then**     ▷ Record the location of the maximum
  - 5:          $P_{\text{peak}} \leftarrow P_r$
  - 6:          $x_{\text{peak}} \leftarrow x_n$
  - 7:          $y_{\text{peak}} \leftarrow y_n$
  - 8:     **end if**
  - 9:      $n \leftarrow n + 1$
  - 10: **end while**
  - 11: **Return** the location of the maximum estimated power  $(x_{\text{peak}}, x_{\text{peak}})$ .
- 

The algorithm's while loop evaluates the power level within the grid in steps 2 and 3. The maximum power level will correspond with the MU-coordinates in the  $xy$ -plane. Once a peak is detected (step 4), the peak position will be stored as in steps 6 and 7. As a result of this loop, the highest peak coordinates will be the one represented in the variables  $x_{\text{peak}}$

and  $y_{\text{peak}}$ ; which is returned in step 11.<sup>1</sup>

Step two is implemented by assuming perfect knowledge of the channel. Although this seems unrealistic at first glance, perfect channel knowledge only requires devising distances and the response description of the IRS's radiation elements. When assuming a free-space channel, the channel gain between the BS and the IRS is evaluated with the prior evaluation of both device locations and antenna gains; similarly, for the link between the IRS and the MU. In the case of the BS-IRS link, the channel gain is given by

$$h_n = \sqrt{\frac{A_u F_n^{tx} F_n^t}{4\pi d_{t,n}^2}} e^{-j2\pi d_{t,n} \frac{1}{\lambda}}, \quad (3)$$

which is dependent on the distance between the BS and the  $n$ -th element of the IRS, on the one hand. On the other hand, this expression is also dependent on the radiators' elements like the aperture of the antenna  $A_u$  and the radiation pattern of the BS and the IRS, as given by  $F_n^{tx}$  and  $F_n^t$ , respectively. Both of these elements are well defined in advance and do not require to be estimated.

Similarly, this occurs for the channel gain between the  $n$ -th element of the IRS and the intended MU. As follows from the expression

$$g_n = \sqrt{\frac{A_r F_n^{rx} F_n^r}{4\pi d_{r,n}^2}} e^{-j2\pi d_{r,n} \frac{1}{\lambda}}, \quad (4)$$

the channel gain is only dependent of the distance  $d_{r,n}$  to the intended MU and properties of the radiator elements as given by the  $F$ 's parameters.

Based on these two expressions, we configure the IRS compensating for the channel as

$$\hat{\theta} = \frac{g_n^* h_n^*}{|g_n h_n|}, \quad (5)$$

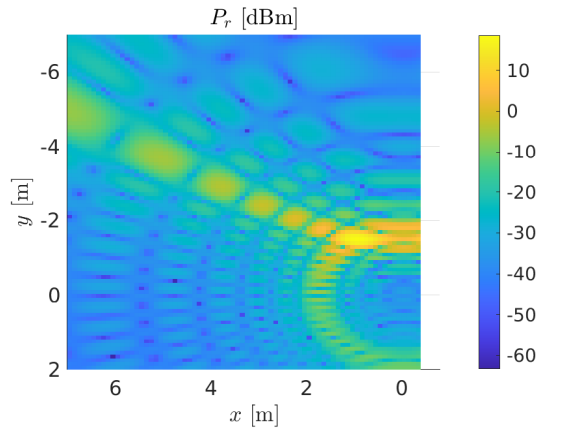
where  $\hat{\theta}$  is the reflection coefficient of the  $n$ -th element in the IRS. In this way, we complete the second step in Algorithm 1. We re-evaluate Eq. (5) for each different block in the grid. Each block only updates the distance term  $d_{r,n}$  for  $g_n$ .

Following this algorithm, the power of the received signal is computed in the third step. The power is readily evaluated in the discrete domain with the expression  $\frac{1}{N} \sum_{n=1}^N r^2(t_n)$ , where  $N$  is the total of samples of the signal and  $t_n$  is the discrete time. To illustrate the impact of the MU location and the channel gains with the IRS, we evaluate this power without noise. In this way, the received power is directly evaluated as

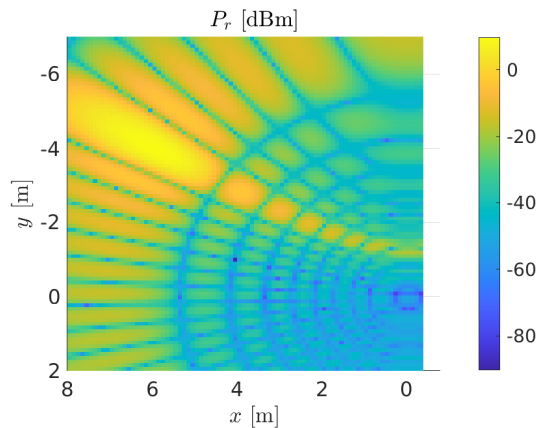
$$P_r = 20 \log_{10}(w) + 30 + P_{\text{MU}} [\text{dBm}]. \quad (6)$$

Next, the peak is located within the **if** condition in code lines 4 to 8. The peak location is updated in the loop with the update of the IRS. Although this is comparable to the brute force algorithm, this is nested in the loop to reconfigure the IRS, which must be implemented in any case. Conceiving a more efficient algorithm to look for the maximum will not save

<sup>1</sup>We provide open access to the code in the link [https://github.com/jorge-torresgomez/IRS\\_localization](https://github.com/jorge-torresgomez/IRS_localization)



(a) Received power level at the BS when the MU is located at coordinates (1, -1.5, 0).



(b) Received power level at the BS when the MU is located at coordinates (6, -4, 0).

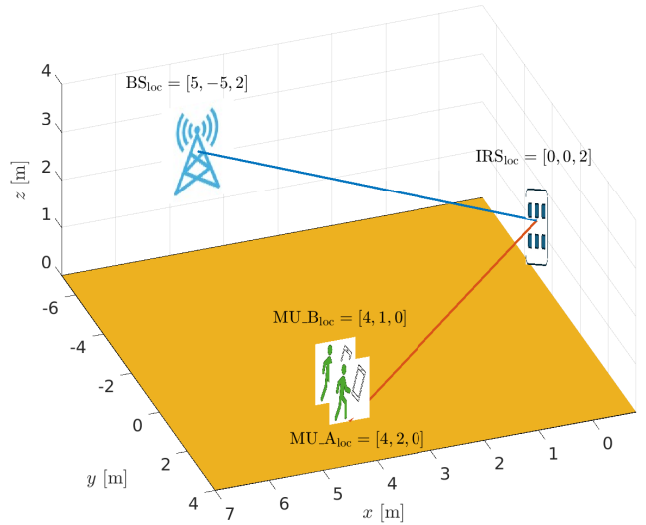
Fig. 2. Power level for two different locations of MU with respect to the IRS.

resources significantly, as it will only replace the `if` condition in Algorithm 1. Finally, the algorithm returns the estimated location of the MU in line eleven with the location of the power's peak.

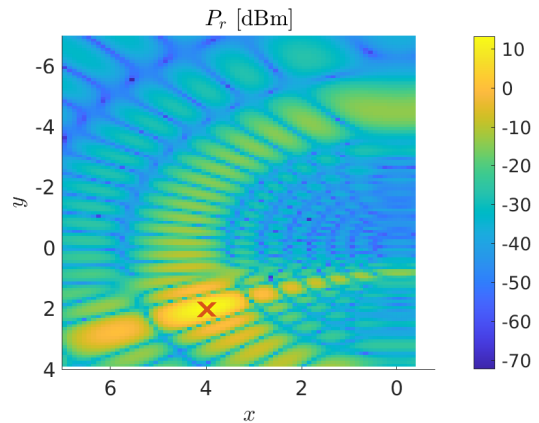
Using this simple solution, the power's peak is estimated more or less accurately depending on the position of the MU position concerning the IRS location. In the close vicinity of the IRS, the location of the peak can be more accurately determined as the resulting IRS's beam can be more focused. On the contrary, when the MU is located farther from the IRS, the error in the IRS location increases. Fig. 2 comparatively illustrates two cases, when the user is located close to the IRS in a) and farther in b) but along the same LoS. As we can observe in this figure, the spreading of the peak increases not only with the distance but also more markedly in the radial direction than in the azimuth.

## V. RESULTS

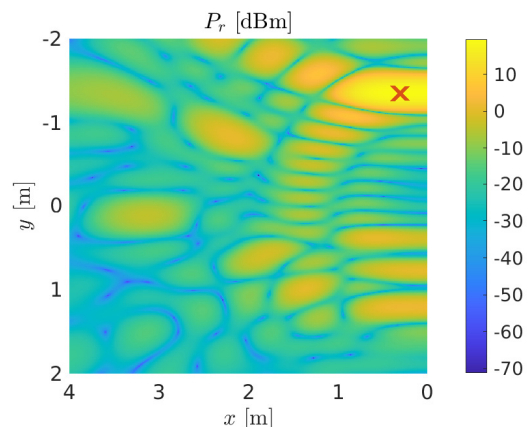
In this section, we investigate on the localization accuracy when other MUs are also performing simultaneous emissions. We implement the communication system with the parameters listed in Table I. We assume all the MUs performs emissions



(a) Schematic representation of two MUs.



(b) Received power level at the BS. The target MU is located at coordinates (1, -1.5, 0) with a second MU as interference.



(c) Received power level at the BS. The MU is located at coordinates (0.5, -1.5, 0) and nine other MUs are producing interference.

Fig. 3. Received power with the deployment of various MUs.

with the same power lever as 30 dBm. We abstract the waveform detection process by evaluating the received power with the coefficient  $w$  in Eq. (6). We evaluate the received power per coordinate location  $(x_n, y_n)$  dividing the area in blocks of dimension  $100 \times 100$  cm. Next, we follow the Algorithm 1 to evaluate the peak power and estimate the location of the target MU.

To model the hardware impairment, we also add to the evaluated power in Eq. (6) the contributions from the neighbors MUs' emissions. We add to the received power from the target MU a fraction of the power from neighbors MUs, as given by the coefficient  $\alpha = 0.1$ . This value of  $\alpha$  contaminates the received signal with the 10% of the power signal from the other emissions. In this way, we model the interference produced by neighbors MUs as performing simultaneous emissions. The impact of two MUs is illustrated in Fig. 3a. After we evaluate the received power at the BS while scanning in the  $xy$ -plane, we will observe two peaks in correspondence with the users' locations A and B, as depicted in Fig. 3b. The strongest peak, marked with the red X, is with the intended target.

The localization of the MU will be less accurate when increasing the number of MUs, as more energy will interfere the link between the target MU and the IRS. This is illustrated in Fig. 3c, where nine other MUs are randomly distributed in the area and perform simultaneous emissions. As depicted in this figure, the power around the target MU looks wider, increasing the localization errors.

Finally, we illustrate in Fig. 4 the magnitude of the localization error with the total of users. The error is measured with the distance between the estimated position of the target MU and the actual one. Although the error looks like oscillating with the MU, it tends to increase with the amount of MU. These oscillations are produced due to the random location of the neighbors MUs in the grid.

## VI. CONCLUSION

This paper elaborates on a low complex method to localize MUs in the ground plane by looking at the power emissions through an IRS-assisted link. The localization runs at the BS,

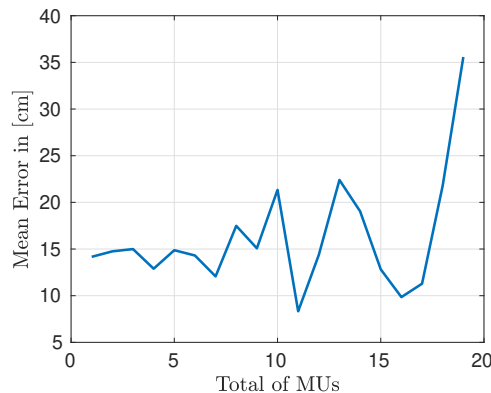


Fig. 4. Absolute error in determining the target's position MU with the total of users.

which NLoS conditions with the target; the BS will look at the location of the peak power to estimate the position of the MU. This solution can be extended to a more concrete communication scheme when integrating the communication pipeline of mobile standards like 5G/6G or the WiFi standard. This integration will account for more realistic hardware impairments in the transmission and reception process. Furthermore, the timeliness of the MU localization can be assessed when including mobility patterns in the system model. In future work, we will assess the information freshness at the BS regarding the actual position of the MU.

## ACKNOWLEDGEMENTS

This work was supported by the Federal Ministry of Education and Research (BMBF, Germany) within the 6G Research and Innovation Cluster 6G-RIC under Grant 16KISK020K.

## REFERENCES

- [1] C. Pan, G. Zhou, K. Zhi, S. Hong, T. Wu, Y. Pan, H. Ren, M. Di Renzo, A. L. Swindlehurst, R. Zhang, and A. Y. Zhang, "An Overview of Signal Processing Techniques for RIS/IRS-Aided Wireless Systems," *IEEE Journal of Selected Topics in Signal Processing*, vol. 16, no. 5, pp. 883–917, Aug. 2022.
- [2] C. L. Nguyen, O. Georgiou, G. Gradoni, and M. Di Renzo, "Wireless Fingerprinting Localization in Smart Environments Using Reconfigurable Intelligent Surfaces," *IEEE Access*, vol. 9, pp. 135 526–135 541, 2021.
- [3] J. Angjo, A. Zubow, and F. Dressler, "Side Effects of IRS: On the Need for Coordination in 6G Multi-Operator IRS-assisted Networks," in *IEEE GLOBECOM 2023, 6GComm Workshop*, Kuala Lumpur, Malaysia: IEEE, Dec. 2023, pp. 1380–1385.
- [4] H. Zhang, B. Di, K. Bian, Z. Han, H. V. Poor, and L. Song, "Toward Ubiquitous Sensing and Localization With Reconfigurable Intelligent Surfaces," *Proceedings of the IEEE*, vol. 110, no. 9, pp. 1401–1422, Sep. 2022.
- [5] A. Elzanaty, A. Guerra, F. Guidi, and M.-S. Alouini, "Reconfigurable Intelligent Surfaces for Localization: Position and Orientation Error Bounds," *IEEE Transactions on Signal Processing*, vol. 69, pp. 5386–5402, 2021.
- [6] Z. Abu-Shaban, K. Keykhosravi, M. F. Keskin, G. C. Alexandropoulos, G. Seco-Granados, and H. Wymeersch, "Near-field Localization with a Reconfigurable Intelligent Surface Acting as Lens," in *IEEE ICC 2021, Virtual Conference: IEEE*, Jun. 2021.
- [7] Y. Lin, S. Jin, M. Matthaiou, and X. You, "Channel Estimation and User Localization for IRS-Assisted MIMO-OFDM Systems," *IEEE Transactions on Wireless Communications*, vol. 21, no. 4, pp. 2320–2335, Apr. 2022.
- [8] J. V. Alegria and F. Rusek, "Cramér-Rao Lower Bounds for Positioning with Large Intelligent Surfaces using Quantized Amplitude and Phase," in *53rd Asilomar Conference on Signals, Systems, and Computers*, Pacific Grove, CA: IEEE, Nov. 2019.
- [9] D. A. Tubail, M. El-Absi, S. Ikki, and T. Kaiser, "Hardware-Aware Joint Localization-Synchronization and Tracking Using Reconfigurable Intelligent Surfaces in 5G and Beyond," *IEEE Open Journal of the Communications Society*, vol. 5, pp. 1899–1915, 2024.
- [10] D. Dardari, N. Decarli, A. Guerra, and F. Guidi, "LOS/NLOS Near-Field Localization With a Large Reconfigurable Intelligent Surface," *IEEE Transactions on Wireless Communications*, vol. 21, no. 6, pp. 4282–4294, Jun. 2022.
- [11] K. Keykhosravi, M. F. Keskin, G. Seco-Granados, and H. Wymeersch, "SISO RIS-Enabled Joint 3D Downlink Localization and Synchronization," in *IEEE ICC 2021, Virtual Conference: IEEE*, Jun. 2021.
- [12] H. Zhang, B. Di, K. Bian, Z. Han, and L. Song, "MetaLocalization: Reconfigurable Intelligent Surface Aided Multi-User Wireless Indoor Localization," *IEEE Transactions on Wireless Communications*, vol. 20, no. 12, pp. 7743–7757, Dec. 2021.
- [13] Y. Cui, H. Yin, L. Tan, and M. Di Renzo, "A 3D Positioning-based Channel Estimation Method for RIS-aided mmWave Communications," arXiv, cs.IT 2203.14636, Apr. 2022.